Fermi-Liquid Parameters of He^3 in the Brueckner Theory*

George F. Bertsch
Palmer Physical Laboratory, Princeton University, Princeton, New Jersey 08540
(Received 3 February 1969)

Functional differentiation of the Brueckner-theory equations gives a prescription for calculating the effective interaction in a Fermi liquid. The many terms that result from the differentiation are calculated for the liquid-He^3 system using Østgaard's reaction matrices. He^3 is strongly interacting in the sense that the defect wave-function probability κ is large, of the order 0.56. As a result, many of the terms contribute substantially to the total. Of the Landau parameters f_0, f_1, and z_0, only z_0 is in reasonable agreement with experiment. The parameter f_0 is too small. This is known to be due in part to the neglect of three-body clusters. We find a small value for f_1, implying that the effective mass m^* is close to one. Larger effective masses could be obtained by treating low-momentum-transfer processes more carefully and by summing higher-order diagrams.

INTRODUCTION

The bulk properties of liquid He^3 can be parametrized by the phenomenological theory of Landau.[1] The parameters required are the diagonal matrix elements of the effective interaction between atoms at the Fermi surface. One would like to calculate bulk properties starting from a realistic interaction between He^3 atoms. This was attempted with reasonable success by Brueckner and collaborators.[2] Several more recent calculations[3,4] follow essentially the same theory, with improved approximations for some higher-order correlations. Another method has been recently described[5] based on cluster expansions techniques.

The Landau parameters are defined as

$$f^{s_1 s_2}(\theta) = \frac{\partial^2 (E/V)}{\partial n_{k_1 s_1} \partial n_{k_2 s_2}}\bigg|_{\hat{k}_1 \cdot \hat{k}_2 = \cos\theta,\ |k_i| = k_F}, \tag{1}$$

$$f_l = \tfrac{1}{2}(2l+1)\int_{-1}^{+1} (f^{\uparrow\uparrow}(\theta) + f^{\uparrow\downarrow}(\theta)) P_l(\cos\theta)\, d\cos\theta, \tag{2}$$

$$z_l = \tfrac{1}{2}(2l+1)\int_{-1}^{+1} (f^{\uparrow\uparrow}(\theta) - f^{\uparrow\downarrow}(\theta)) P_l(\cos\theta)\, d\cos\theta.$$

In Eq. (1), the total system energy per unit volume is varied with respect to the number of particles per unit volume. The k and s are momentum and spin indices of the particles. The parameters are connected with the experimentally measured sound velocity, specific heat, and magnetic susceptibility by[6]

$$s^2 = (\hbar^2 k_F^{\,2}/3m^2)(1 - \tfrac{1}{3}\tilde{f}_1 + \tilde{f}_0),$$
$$c_v = (m^* k_F/3\hbar^2)K^2 T, \quad m/m^* = (1 - \tfrac{1}{3}\tilde{f}_1), \tag{3}$$
$$\mu^2/\chi = (\pi^2\hbar^2/m k_F)(1 + \tilde{z}_0).$$

Here $\tilde{f}$ and $\tilde{z}$ are the interactions in the dimensionless units $\tilde{f} = [(k_F/2\pi^2)(m/\hbar^2)]f$.

It has recently been shown that most of the effective mass comes from low-energy correlations.[7] In this situation, it is more useful to work with particles not dressed with the correlations. Schrieffer and Berk[8] thereby obtain an expression for the susceptibility which does not use the low-energy contribution to f_1.

Naively, one would expect to be able to make a direct association between the Landau-interaction parameters and the Brueckner effective interaction $\langle k_1 k_2 | G | k_1 k_2 \rangle$. It is easy to see that the relationship is actually more complicated[9] by noting that the prediction of a theory for the Landau parameters is made by substituting the expression for the energy of the theory in Eq.(1). Thus, only in the Hartree-Fock approximation would there be a direct correspondence between the effective interaction and the two-body force.

When using the Brueckner theory, only the combination of parameters giving the compressibility and sound velocity is straightforward to calculate. This is because the variation is with respect to density, and the density is a natural parameter of the theory, entering via k_F, the Fermi momentum. One simply computes the total energy for various densities and differentiates numerically. Unfortunately, the other parameters are not so easy to get at by numerical differentiation. Brueckner estimated f_1 from the G matrix alone and z_0 from several of the terms in $\partial^2(E/V)/\partial n_1 \partial n_2$.[10]

In this paper, we shall make a complete diagrammatic expansion of the Brueckner theory to find the contributions to the Landau parameters. It is then possible to make a consistent calculation of all the parameters measurable in Eq. (3). It is particularly interesting that calculations done of the specific heat (Ref. 7) find a large value of f_1 from a class of diagrams but assume

that there is already a large f_1 from the Brueckner diagrams. It would also be interesting to compute z_1 and f_2, which may also be measurable.[11,12]

REVIEW OF BRUECKNER THEORY

In the Brueckner theory, the two-body wave function is determined from the Bethe-Goldstone equation

$$\Psi_{k_1k_2}(r) = \Phi_{k_1k_2}(r) - \int_{k_3,k_4>k_F} \frac{d^3K}{(2\pi)^3} e^{-iKr} \times \int (d^3r') \frac{e^{iKr'} V(r') \Psi_{k_1k_2}(r')}{e_{k_3}+e_{k_4}-e_{k_1}-e_{k_2}} , \quad (4)$$

where $k_3, k_4 = \frac{1}{2}(k_1+k_2) \pm K$ and $\Phi_{k_1k_2}(r) = \exp[i(k_1+k_2)r]$. From this wave function, the G matrix is defined as

$$G_{k_3k_4}^{\ \ k_1k_2} = \int d^3r \, \Phi^*_{k_3k_4}(r) V(r) \Psi_{k_1k_2}(r) . \quad (5)$$

In practice, partial waves are calculated separately, giving the partial-wave G matrix

$$G_l = \int j_l(kr) V(r) u_l(r) r^2 dr .$$

The choice of intermediate-state energies e_k is a sensitive point, because it involves the correlations of a particle with others while it is interacting with a second. Recent treatments of three-body clusters lead to the prescription that hole energies are to be purely kinetic,[13] i.e.,

$$e_k(\text{particle}) = (\hbar^2/2m)k^2 , \quad (6)$$

$$e_k(\text{hole}) = (\hbar^2/2m)k^2 + \Delta_k , \quad (7)$$

$$\Delta_k = \sum_{\text{spin } i} \frac{d^3k_i}{(2\pi)^3} G_{kk_i}^{\ \ kk_i} . \quad (8)$$

After these equations have been solved self-consistently, the system energy may be calculated as

$$\frac{E}{V} = \frac{1}{2} \sum_{\text{spin } i,j} \int_{k_1,k_2<k_F} \frac{d^3k_1}{(2\pi)^3} \frac{d^3k_2}{(2\pi)^3} G_{k_1k_2}^{\ \ k_1k_2} . \quad (9)$$

The usual set of units for these equations has °K for E and °K Å for G. Following Østgaard, we divide by $\hbar^2/m = 16.36$ °K Å^2 so the units become Å for G and Å^{-2} for E. Landau's dimensionless units are related to these by $2\pi^2/k_F \sim 25.0$ Å.

In the Appendix, we take the functional derivations of (E/V) with respect to particle number.

The equation for f, Eq. (A7), has 13 different terms. These terms can be represented by graphs in the usual way. The interacting particles 1 and 2 are denoted by external lines and intermediate states by closed lines. A G-matrix interaction appears as a wavy line. A new symbol is needed for the hole-energy derivative $\partial\Delta_i/\partial n_j$. We use a dark triangle for this to indicate that it is not symmetric between i and j, and also, that many elementary graphs are summed to give the self-consistent interaction $\partial\Delta_i/\partial n_j$. The equations for the hole interaction [Eqs. (A8) and (A9)] are integral equations. Once this interaction is obtained, the equation for f [Eq. (A7)] is simply perturbation theory.

The graphs representing all but the last term in Eq. (A7) are given in Figs. 1 and 2. The four graphs in Fig. 1 are simpler in that they do not involve the self-energy. We now discuss these term by term, starting with the G matrix itself [Fig. 1(a)].

G-MATRIX

The G-matrix elements we use were calculated by Østgaard[3] from the Yntema-Schneider potential. This calculation treated the c.m. in an average way, which appears to be a reasonable approximation. The Fermi momentum was taken at $k_F = 0.78$ Å^{-1}, which gives near self-consistency[14] for the hole energy with $m^* = 1.0$ and $\Delta = 0.4$. The G matrix in the range required for calculating f is quoted in Table I up to the $L = 2$ partial wave.

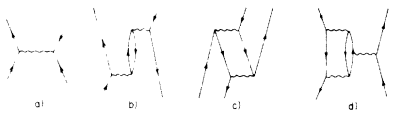

FIG. 1. Some graphs contributing to the particle-hole interaction in the Brueckner theory. These are the simplest graphs: All remaining contributions involve the self-consistent hole energies of Brueckner theory.

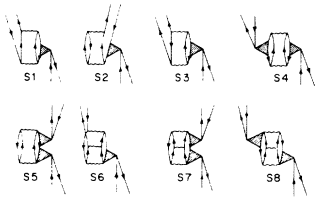

FIG. 2. Graphs with first derivatives of the hole energy, which are required for a complete calculation of the Landau parameters in the Brueckner theory.

TABLE I. G-Matrix Elements. The Fermi momentum and hole energy are taken as $k_F = 0.78$, $\epsilon_{\text{hole}} = (\hbar^2/2m) \times (k^2 - 0.4k_F^2)$. Each set of three entries in the table gives, respectively, the S-wave, P-wave, and D-wave parts.

$\left(\frac{k}{k_F}\right)_{\text{out}}$	$(k/k_F)_{\text{in}}$ 0.0	0.25	0.50	0.75	1.00
0.0	4.2	16.2	31.7	42.9	43.8
0.25	18.7	27.0	37.8	44.9	42.8
		−13.6	−17.6	−12.6	−4.5
		−1.5	−3.8	−4.3	−3.7
0.50	42.1	44.6	47.3	47.7	41.7
		−17.4	−24.2	−18.4	−5.5
		−3.8	−10.5	−13.7	−12.4
0.75	63.5	62.0	57.8	50.8	40.2
		−11.3	−16.5	−12.0	0.0
		−4.2	−13.5	−20.7	−20.9
1.00	75.2	71.7	64.0	52.1	37.4
		−1.4	−0.5	+4.0	11.9
		−3.5	−12.2	−20.7	−23.1
1.25	74.1	70.0	61.4	48.7	33.2
		+8.8	16.8	23.3	27.6
		−2.3	−7.8	−13.8	−15.8
1.50	61.9	58.3	51.1	40.1	26.9
		16.6	30.4	39.2	41.4
		−0.6	−2.1	−3.3	−2.3
1.75	41.7	39.4	34.7	27.4	18.5
		20.3	36.9	47.2	43.6
		1.0	3.6	7.8	13.1
2.00	19.1	18.2	16.3	13.2	9.3
		20.0	36.6	46.8	48.2
		2.2	8.3	17.0	26.5

The G matrix is given in terms of the particle-particle symmetry; to convert to the particle-hole form of the Landau parameters, use definition (2) and

$$f^{\uparrow\uparrow} = 2G(\text{odd}) = 2\sum_{l\ \text{odd}} (2l+1)G_l\,,$$
$$f^{\uparrow\downarrow} = G(\text{even}) + G(\text{odd}) = \sum_l (2l+1)G_l\,, \tag{10}$$

$$\text{giving} \quad f(a) = G_e + 3G_0, \quad z(a) = G_0 - G_e\,. \tag{11}$$

For the more complicated graphs considered later, it is also convenient to use Racah algebra to recouple the spin from the particle-particle channel to the particle-hole channel.

The G matrix by itself has strong components of multipole order 0, 1, and 2, as may be seen from Fig. 3. The strength of the 0 and 1 multipoles is given in the first row of Table II. The contributions to both f_0 and f_1 are the wrong sign, as is the case in Ref. 6, Fig. 5. The contribution to z_0 is strong enough to induce ferromagnetic instability. Brueckner's original calculation gave a contribution to f_1 of the proper sign, probably because of the different energy denominator he used.

CORE-EXCITATION GRAPH

The second term in Eq. (A7), which is depicted in Fig. 1(b), gives the interaction of two particles via an excitation of the Fermi sea. The main physical effect of the graph is to include the interference of a valence particle with a core excitation. Therefore, the graph is mostly repulsive. Physically, there is also an attractive part corresponding to the coherent spatial polarization of the Fermi sea, as in electron screening.

TABLE II. Contribution of Brueckner-theory graphs to Fermi liquid parameters. Graphs are shown in Fig. 1. The interaction parameters are in units of $2\pi^2\hbar^2/k_F m$.

Graph	f_0	f_1	z_0	z_1
a	−0.95	−0.57	−1.75	−0.54
b	2.93	0.13	−0.04	0.71
	(17.0)	(2.8)		
c	−0.27	0.44	0.26	−0.44
	(−0.97)	(1.34)		
d	0.97	−0.08	0.52	0.34
Self-energy insertions	−1.14	−0.04	−0.18	0.01
Total	1.54	−0.12	−1.71	0.08
Experimental (Ref. 6)	3.5	2.0	−0.9	

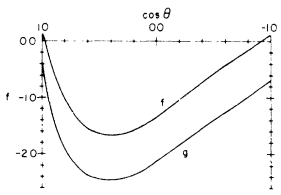

FIG. 3. Interaction between particles on the Fermi surface due to the G matrix, Fig. 1(a). The strength of the interaction is in units $[(m/\hbar^2)(k_F/2\pi^2)]$, and Θ is the angle between the momentum vectors of the two particles taken from the center of the Fermi sphere. Compare Fig. 4, Ref. 4.

This is most prominent in nonforward scattering matrix elements but is also present in the attractive part of the contribution to z [Eq. (14)].

With the spin sums and external factor of 4 required by Eq. (A7), the detailed expression for the graph is

$$f(b) = 4\int [d^3k/(2\pi)^3] E^{-1}(G_e^{\,2} + 3G_0^{\,2}),$$
$$z(b) = 8\int [d^3k/(2\pi)^3] E^{-1}(G_0^{\,2} + G_e G_0). \tag{12}$$

In this equation and the similar ones below, the integration is over all internal hole lines. Because of possible collective effects in the intermediate particle-hole bubble, it is also worthwhile to express the graph in a form with definite symmetry of the intermediate particle-hole wave function

$$f(b) = \int [d^3k/(2\pi)^3] (F^2 + 3Z^2),$$
$$z(b) = \int [d^3k/(2\pi)^3] (-Z^2 + F^2), \tag{13}$$

with $F = G_e + 3G_0$, and $Z = G_0 - G_e$.

Just from the signs here, it may be seen that a repulsive f and an attractive z are both enhanced in higher order.[15]

Computation of this graph requires G matrices with incoming momentum in the range $0 < k < k_F$ and outgoing momentum in the larger range $0 < k < 2k_F$. The integral is easy to evaluate by computer; a 225-point mesh gave accuracy better than 1% for the three-dimensional phase-space integral. The result for the interaction f is plotted as the full line in Fig. 4. For any force, f is repulsive, as can be seen immediately from Eq. (12).

We also find that f drops to zero in the forward direction. This is a consequence of the asymmetric treatment of the energy denominator: Although the phase space goes to zero as the momentum transfer decreases, the energy denominator would also vanish with a symmetric treatment and give a finite limit for the contribution of the graph.

In the paramagnon models of Berk and Schrieffer and Doniach and Engelsberg,[7] it is just the behavior of this process in the forward direction that gives the large effective mass observed at the lowest temperatures. They calculate the effective mass by summing the graphs of the type shown in Fig. 5(a) and finding the momentum dependence. This is completely equivalent[16] to calculating the parameter f_1 with the graphs of type Fig. 5(b). In their picture, f is sharply peaked in the forward direction. This gives a repulsive f_1 and also affects f_0 so that $\delta f_0 \sim \delta f_{1/3}$. Thus, from Eq. (3), we see that the compressibility, or equivalently the speed of sound, is not affected by these low-momentum processes.

Because of the great sensitivity of f_1 to the treatment of low-momentum effects, we also computed the Brueckner-theory graph Fig. 1(b) setting the energy gap Δ equal to zero. This is shown by the broken curve in Fig. 3. We now get a finite contribution at $\cos\theta \simeq 1$ but by no means the forward peaking found in the paramagnon picture. The difficulty is that there are also singularities arising from the part of phase space corresponding to forward scattering in the crossed channel.[17] Just by exchanging particles, a low-momentum-transfer singularity becomes a singularity for some high-momentum-transfer process.

The multipole contributions to f and g in the Brueckner theory are tabulated on the second line of Table II. Most of the experimental f_0 comes from this graph. As mentioned above, f_1 comes out small because of the energy gap. When calculated without the energy gap, f_1 is much larger, as indicated in parentheses in the table.

OTHER G-MATRIX GRAPHS

The hole-hole correlation, Fig. 1(c), is attractive with the same spin sums as for particle-particle scattering

$$f(c) = -\int [d^3k/(2\pi)^3] E^{-1}(G_e^{\,2} + 3G_0^{\,2}),$$
$$z(c) = \int [d^3k/(2\pi)^3] E^{-1}(G_e^{\,2} - G_0^{\,2}). \tag{14}$$

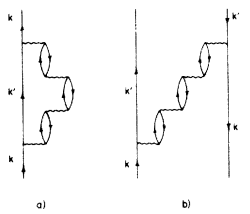

FIG. 4. Spin-symmetric interaction between particles on the Fermi surface due to the rearrangement term Fig. 1(b). Solid line is Brueckner-theory result; dashed line is computed the same way but with no energy gap.

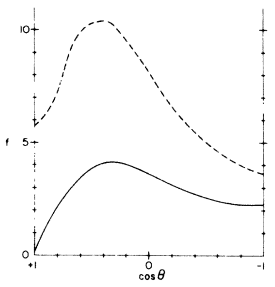

FIG. 5. Higher-order diagrams not in the Brueckner theory needed to obtain the very large effective mass at low temperature. The graph (a) is a self-energy modification of the single-particle Green's function calculated in Ref. 9. The equivalent graph in the Landau theory is (b).

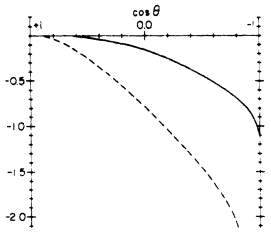

FIG. 6. The spin-symmetric interaction f between particles on the Fermi surface due to the hole-hole correlation, graph (c) in Fig. 1. Solid line is result of Brueckner theory, and dashed line is computed without the energy gap.

In what is called the T-matrix approximation,[9] this graph and further iterations are included along with the particle-particle correlations in defining the basic interaction. It could be important to include higher iterations because there can be a singularity for low-momentum transfer. Low-momentum-transfer processes give an attraction at the point $\cos\theta = -1$ and contributes this to f_1 with the proper sign and to f_0 with the wrong sign. As in the previous case, the value for f_1 depends critically on the energy denominator for small momentum transfer. However, even with an energy gap there is a sizable contribution to f_1, as may be seen from Fig. 6 and the third row of Table II.

The next graph [Fig. 1(d)] has the sign of the intermediate interaction. This is an off-energy-shell interaction, which is larger and more repulsive than the G matrix of Table I for the same incoming and outgoing momenta. Denoting the off-energy-shell interaction by G', the expressions for the graphs are

$$f(d) = \int \frac{d^3k_1}{(2\pi)^3}\frac{d^3k_2}{(2\pi)^3}\frac{1}{E}\frac{1}{E'}(4G_e^{\,2}G_e' + 12G_0^{\,2}G_0'), \tag{15}$$

$$z(d) = \int \frac{d^3k_1}{(2\pi)^3}\frac{d^3k_2}{(2\pi)^3}\frac{1}{E}\frac{1}{E'}[4G_0^{\,2}(G_e' + 2G_0') + 4G_e^{\,2}G_0'].$$

The graph may be interpreted as follows: When a particle is added at k_1, the probability of other particle orbits being occupied increases because the core particles which would normally correlate at k_1 part of the time must correlate elsewhere. Therefore, it is more difficult to add a particle at some other point, and the effective interaction is repulsive. As is reasonable from this argument, the contribution to f is very smooth as a function of angle.

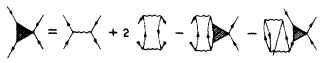

FIG. 7. Graphical representation of Eq. (A8).

SELF-ENERGY INSERTIONS

Before computing the terms in Eq. (10) with hole interactions, we must solve Eqs. (A7)–(A9) for the hole interactions. The integral equation for $\partial\Delta_1/\partial n_2$ can be expressed diagramatically as in Fig. 7. The inhomogeneous part of this equation gives the hole energy as the sum of the interaction energy and the rearrangement energy. By the Hugenholtz-Van Hove theorem,[18] this should be negative on the average. In fact, the two terms give an average repulsion because we have not chosen a self-consistent k_F. Thus, the signs of the contributions we calculate for f from the insertions will be suspect.

To better understand the structure of the above equation, spin sums can be performed and a multipole expansion made in terms of the angle between the momentum vectors of the two particles. This yields a set of equations for the different spins and multipolarities, depending on a function of only one variable, the length of the hole momentum vector

$$\Delta_{ls}(k) = \Delta_{ls}^{(0)}(k) - [4\pi/(2l+1)](2\pi)^{-3}\int_0^{k_F} k'^2 dk' K_{ls}(k,k')\Delta_{ls}(k') - \Delta_{ls}(k)\int [d^3k'/(2\pi)^3 K_{00}(k,k'), \tag{16}$$

where we have defined

$$\Delta_{ls}(k) \equiv \tfrac{1}{2}(2l+1)\int_{-1}^{+1} d\cos\theta_{12} P_l(\theta_{12})\left(\frac{\partial\Delta_{1\uparrow}(k)}{\partial n_{2\uparrow}} + (-1)^s\frac{\partial\Delta_{1\uparrow}(k)}{\partial n_{2\downarrow}}\right), \tag{17}$$

$$K_{ls}(k,k') = \iint_{\text{particles}} \frac{d^3k_p}{(2\pi)^3}\frac{1}{E^2}[(G_{kk'}{}^{k_p k_p'})^2 + (-1)^s(G_{kk'}{}^{k_p k_p'})^2]\frac{2}{2l+1}P_l(\cos\theta)d\cos\theta_{kk'}, \tag{18}$$

$\Delta^{(0)}\sim$ inhomogeneous part of Eq. (A8). (19)

There are two pieces to the kernel of this equation. The last term just multiplies Δ by a number, and therefore will cut down all the multipoles by some constant factor. Neglecting the second term in Eq. (18)

for the moment, the solution is

$$\Delta_{ls}(k) = [1 + \overline{K}_{00}(k)]^{-1} \Delta_{ls}{}^{(0)}(k), \quad \text{with } \overline{K}_{ls}(k) = \int [d^3k'/(2\pi)^3] K_{ls}(k,k') . \tag{20}$$

The physical interpretation of this factor is that the strength of the hole has been renormalized by the possibility of virtual excitation. The integral of the kernel is closely related to the defect wave-function probability of Brandow [19]

$$\kappa_{\text{Brandow}} = \overline{K}_{00} = \rho \int [d^3k_p/(2\pi)^3][\tfrac{1}{2}G_e{}^2 + \tfrac{3}{2}G_0{}^2)/E^2] . \tag{21}$$

This is the lowest-order probability for a given hole orbit being empty. By considering more graphs than the Brueckner theory yields, Brandow obtains a renormalization factor

$$P = 2/[1 + (1 + 4\overline{K}_{00})^{1/2}] . \tag{22}$$

Østgaard's G matrices yield the value[20] $\overline{K} = 0.56$ for a hole at $k_F = 0$, to be compared with $\overline{K} = 0.25$ for nuclear matter.[21] Thus, He^3 is a much more strongly interacting than nuclear matter.

For the Brueckner theory, the kernel $K(k,k')$ is smooth as a function of hole momentum, as may be seen from Tables XI, XII, and XIII of Ref. 6. So in practice, the kernels can be taken as constants and Eq. (A8) solved as an algebraic equation. This would no longer be the case in a theory without the energy gap.

For numerical evaluation of the function $K_{ls}(k,k')$, it was not convenient to integrate k_p over all momentum space. We instead used the relation

$$\int [d^3k_p/(2\pi)^3] (G/E)^2 = \tfrac{1}{2}(\partial G/\partial \Delta) . \tag{23}$$

This requires $\partial G/\partial \Delta$, which was obtained numerically from Østgaard's tables and is plotted in Fig. 8. The results for the integrals are quoted in Table III.

The hole interaction with the approximation $K_l(k,k')$ = constant is

$$\Delta_{ls}(k) = [1 + (2l+1)^{-1}\overline{K}_{ls} + \overline{K}_{00}]^{-1} \Delta_{ls}{}^{(0)}(k) . \tag{24}$$

Numerical values are given in Table IV. The spin symmetric interaction is small from the cancellation of the two terms in $\Delta^{(0)}$. The spin antisymmetric interaction is large, implying that the higher-order graphs [Eq. (A7)] will be important.

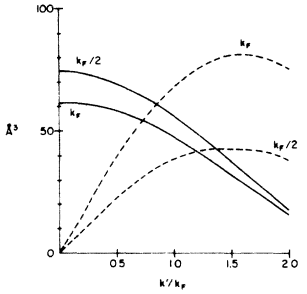

FIG. 8. The derivative of the G matrix with respect to the single-particle energy. Graphs are shown for hole relative momentum $\frac{1}{2}k_F$ and k_F, as a function of particle relative momentum. Solid line is $\partial G_s/\partial e_i$ and broken line is $3\partial G_p/\partial e_i$. Units are Å^3.

TABLE III. Integrals of hole probability $\overline{K}_{LS}$.

	Multipolarity	
	$L=0$	$L=1$
Spin $S=0$ (f)	0.56	−0.07
$S=1$ (z)	−0.34	0.12

TABLE IV. Self-consistent hole interaction computed with Eq. (25) and averaged over all holes. Units are dimensionless as with f and z.

	Multipolarity	
	$L=0$	$L=1$
Spin $S=0$	0.23	−0.34
$S=1$	−1.73	0.25

CONTRIBUTIONS TO f FROM HOLE SELF-ENERGIES

There are eight terms in the expansion for f that involve the first-order derivative of self-energies. These terms are shown graphically in Fig. 2. The first two graphs $S1$ and $S2$ involve valence-hole lines, and are easily computed within our previous approximation

$$f_{ls}(S1) = -[2/(2l+1)]\overline{K}_{ls}\,\overline{\Delta}_{ls}\,, \tag{25}$$

$$f_{ls}(S2) = -2\overline{K}_{00}\overline{\Delta}_{ls}\,. \tag{26}$$

These expressions include the factor of 2 from Eq. (A7). The second term is just a renormalization of the hole strength in f. Both these graphs give large contributions tabulated in Table V.

The third self-energy graph $S3$ has a valence-particle line. Defining the probability of a particle orbit being full

$$K_{+}(k_1) = \int [d^3k_i/(2\pi)^3][d^3k_j/(2\pi)^3]\{[G_{ij}^{\ lm}(\text{even})]^2 + 3[G_{ij}^{\ lm}(\text{odd})]^2\}(E^{-2})\,, \tag{27}$$

where $k_i, k_j < k_F$ and $k_m > k_F$. This graph contributes to f_0

$$f_{ls}(S3) \approx [4/(2l+1)]\overline{K}_{+ls}\,\overline{\Delta}_{ls}\,. \tag{28}$$

Numerically, $\overline{K}_{+}(00) \simeq 0.12$ when calculated from the definition Eq. (29). This is probably too small; we should have the equality

$$\int_{k_F}^{\infty}[d^3k_j/(2\pi)^3]K_{+}(k_j) = \int_0^{k_F}[d^3k_j/(2\pi)^3]K_{00}(k_j) \tag{29}$$

to conserve the number of particles. This does not hold because the G matrices were not calculated with the exact Pauli principle.

The remaining graphs in Fig. 6 are of higher order and tend to be small. The expressions used to estimate these graphs are

$$f_{ls}(S4+S5) \approx [2/(2l+1)][\overline{K}_{00} + (2l+1)^{-1}\overline{K}_{ls}]\,\overline{\Delta}_{ls}{}^2\tfrac{1}{2}\rho < E^{-1}\,,$$

$$f_{ls}(S6) = [2/(2l+1)](\rho/2)\overline{\Delta}_{ls}\left[\int \frac{\partial G_{2j}^{\ jm}}{\partial e_2}\,\frac{1}{E}\,G_{jm}^{\ 2j}\right]_{ls}\,, \tag{30}$$

$$f_{ls}(S7+S8) = \frac{2}{(2l+1)}[(\rho/2)\overline{\Delta}_{ls}]^2\left\{\frac{1}{2l+1}\left(\int \frac{\partial G_{12}^{\ mm'}}{\partial e}\,\frac{1}{E}\,G_{mm'}^{\ 12}\right)_{ls} + \left(\int \frac{\partial G_{12}^{\ mm'}}{\partial e}\,\frac{1}{E}\,G_{mm'}^{\ 12}\right)_{00}\right\}.$$

The average intermediate-state energy denominator was found to be

$$\langle E' \rangle \approx (1/1.38)\ \text{Å}^2\,, \tag{31}$$

showing that the particles are most likely to be excited to just above the Fermi sea.

SECOND-ORDER SELF-ENERGY INSERTIONS

The last term in f is

$$f = \frac{d^3k_i}{(2\pi)^3}\frac{d^3k_j}{(2\pi)^3}K(k_i,k_j)\frac{\partial\Delta(k_i)}{\partial n_1 \partial n_2}\,, \tag{32}$$

where both integrations are over hole momenta. Now, since this has an integral over the hole momentum k_i, we can within our approximation integrate over i in the equation defining $\partial\Delta(k_i)/\partial n_1 \partial n_2$, Eq. (A9). The second-order self-energy can then be eliminated, giving

$$f = [-\overline{K}_{00}/(1+2K_{00})]\{f(b) + 2[f(c) + f(d) + f(S4+S5) + f(S6) + f(S7+S8)]\}\,. \tag{33}$$

This is a renormalization of all previous graphs

TABLE V. Contributions to f in Brueckner theory with self-consistent hole energies. The graphs are shown in Fig. 6.

Graph	f_0	f_1	z_0	z_1
$S1$	−0.25	−0.02	−1.21	0.02
$S2$	−0.25	0.37	1.87	0.27
$S3$	0.13	−0.01	−0.08	0.05
$S4$			0.30	
$S5$			−0.48	
$S6$	0.38	0.04	0.07	−0.03
$S7$			−0.01	
$S8$			0.01	
Second order self-energy graph	−1.15	−0.42	−0.65	−0.30
Total	−1.14	−0.04	−0.18	0.01

proportional to the number of internal hole lines they contain. The effect is sizable with $\overline{K}_{00} \approx 0.56$ as may be seen from the entry in Table III.

It is interesting to note that for very large $\overline{K}_{00}$, the net contribution to f from all graphs becomes

$$f = f(a) + \tfrac{1}{2} f(b) , \tag{34}$$

i.e., only the G matrix itself and the core polarization graph contribute when the probability that a hole is empty becomes large.

CONCLUSION

The Brueckner theory of the Landau parameters [Eqs. (1) and (9)] gives a complicated set of expressions for the parameters. However, it is encouraging that numerically, only a few effects which are physically evident are important in the results. The first graphs give strong contributions but have simple interpretations. Most of the self-energy graphs are negligible, except insofar as they renormalize the hole strength.

To compare with experiments, we take the F parameters at 0.28 atm from Ref. 6, and re-express them in terms of the unrenormalized $\tilde{f}$ in Eq. (3). However, we have not included f_1 in the determination of $\tilde{z}_0$ from the magnetic susceptibility, following Ref. 8. Agreement with the Brueckner theory is poor. The parameter f_0 is half of its experimental value. The worst discrepancy is with f_1, which is small and of the wrong sign. We consider that all of these parameters stand on an equal footing, so that if one is off, agreement for another must be fortuitous.

Much of the trouble can be traced to the energy gap which artificially damps virtual excitations at low energy. To justify the gap for a calculation of the ground-state energy, it is noted that terms neglected with the gap can be included at some later stage by calculating three-body clusters. These three-body clusters then give a small contribution to the total energy. However, even though the energy of the three-body cluster might be small, its derivatives with respect to particle number need not be.

Several ways are possible to improve the calculation. If we just use the G matrix as it is in a random-phase-approximation perturbation calculation to lowest order, we would again get the graphs in Fig. 1(a)–1(c) but without the energy gap. Table II shows that this would have a large effect of the right order of magnitude to explain the discrepancy.

More systematically, Brandow suggests dividing the phase space into a core part and a valence part and using perturbation theory in the valence band. Although simple in principle, this method has a practical difficulty in separating the valence contribution from the high-energy contribution in a term such as the graph in Fig. 1(b). It might also be possible to make some explicit calculation of the three-body clusters. There would be very many terms, most of which would be negligible. Without better understanding, a formal functional differentiation of the three-body cluster equations would be very laborious. Finally, it might be useful to return to Brueckner's original scheme and use particle energies defined with off-energy-shell G matrices.

ACKNOWLEDGMENTS

The author is indebted to G. E. Brown for many stimulating conversations and to E. Østgaard for the G-matrix elements needed here. The author is grateful to H. Picker for helpful comments on the manuscript.

APPENDIX

Landau's parameters require the second functional derivative of the total energy with respect to particle number. From the definition Eq. (9), we find for the first derivative

$$\frac{\partial(E/V)}{\partial n_1} = \sum_{s_j} \int_{\text{holes}} \frac{d^3k_j}{(2\pi)^3} G_{1j}^{1j} + \tfrac{1}{2} \sum_{s_i s_j} \int_{\text{holes}} \frac{d^3k_i}{(2\pi)^3} \frac{d^3k_j}{(2\pi)^3} \frac{\partial G_{ij}^{ij}}{\partial n_1} . \tag{A1}$$

To find $\partial G/\partial n$, Eqs. (4) and (5) are formally combined to

$$G = V - V(Q/E)G, \text{ where } Q \text{ is Pauli operator,}$$

$$\text{and} \quad E = (\hbar^2/2m)(k_p^{\,2} + k_{p'}^{\,2} - k_h^{\,2} - k_{h'}^{\,2}) - \Delta_h - \Delta_{h'} , \tag{A2}$$

$$G = (1 + VQ/E)^{-1} V . \tag{A3}$$

The potential V has no implicit dependence on particle number, so differentiating Eq. (A2) gives

$$\frac{\partial G}{\partial n} = -V\frac{\partial(Q/E)}{\partial n}G - V\frac{Q}{E}\frac{\partial G}{\partial n}\,. \tag{A4}$$

Following Ref. 22, we now use Eq. (A3) to solve for $\partial G/\partial n$.

$$\frac{\partial G}{\partial n} = -G\frac{\partial(Q/E)}{\partial n}G\,. \tag{A5}$$

With the indices and integrations explicit this is

$$\frac{\partial G_{kl}^{\ ij}}{\partial n_1} = 2G_{kl}^{\ m1}\frac{1}{E}G_{m1}^{\ ij} - \int_{k_{m'},k_{m''}>k_F}\frac{d^3k_{m'}}{(2\pi)^3}G_k^{\ m'm''}\left(\frac{1}{E}\right)^2 G_{m'm''}^{\ ij}\left(\frac{\partial\Delta_i}{\partial n_1}+\frac{\partial\Delta_j}{\partial n_1}\right)\,, \tag{A6}$$

where $k_1+k_m=k_i-k_j$ and $k_{m'}+k_{m''}=k_i+k_j$.

To get the equation for f, substitute (A6) into (A1) and differentiate once more. To abbreviate the result, we collect terms that are equal and leave the integrations implicit. For the purpose of integration, particle orbits are labeled by m,n and hole orbits by i,j.

$$\begin{aligned}\frac{\partial^2 E}{\partial n_1\partial n_2} &= G_{12}^{\ 12} + 4G_{i2}^{\ m1}\frac{1}{E}G_{m1}^{\ i2} - G_{ij}^{\ 12}\frac{1}{E}G_{12}^{\ ij} + 4G_{ij}^{\ m2}\frac{1}{E}(G_{m2}^{\ n1})'\frac{1}{E}G_{n1}^{\ ij}\\
&- 2G_{i2}^{\ mm'}\frac{1}{E}G_{mm'}^{\ i2}\left(\frac{\partial\Delta_1}{\partial n_1}+\frac{\partial\Delta_2}{\partial n_1}\right) - 8G_{ij}^{\ mm'}\frac{1}{E^2}(G_{mm'}^{\ n1})'\frac{1}{E}G_{n1}^{\ ij}\frac{\partial\Delta_1}{\partial n_2}\\
&+ 4G_{ij}^{\ m1}\frac{1}{E^2}G_{m1}^{\ ij}\frac{\partial\Delta_i}{\partial n_2} + 2G_{ij}^{\ mm'}\frac{1}{E^2}(G_{mm'}^{\ nn'})'\frac{1}{E^2}G_{nn'}^{\ ij}\frac{\partial\Delta_i}{\partial n_1}\left(\frac{\partial\Delta_i}{\partial n_2}+\frac{\partial\Delta_j}{\partial n_2}\right)\\
&- 2G_{ij}^{\ mm'}\frac{1}{E^3}G_{mm'}^{\ ij}\frac{\partial\Delta_i}{\partial n_1}\left(\frac{\partial\Delta_i}{\partial n_2}+\frac{\partial\Delta_j}{\partial n_2}\right) - G_{ij}^{\ mm'}\frac{1}{E^2}G_{mm'}^{\ ij}\frac{\partial^2\Delta_i}{\partial n_1\partial n_2}\,.\end{aligned} \tag{A7}$$

The terms of third order involve off-energy-shell interactions denoted by primes. To find $\partial\Delta_i/\partial n_1$ and $\partial^2\Delta_i/\partial n_1\partial n_2$, we must satisfy the equations obtained by differentiating Eq. (8).

$$\frac{\partial\Delta_i}{\partial n_1} = G_{i1}^{\ i1} + 2G_{ij}^{\ m1}\frac{1}{E}G_{m1}^{\ ij} - G_{ij}^{\ mm'}\frac{1}{E^2}G_{mm'}^{\ ij}\left(\frac{\partial\Delta_i}{\partial n_1}+\frac{\partial\Delta_j}{\partial n_1}\right) \tag{A8}$$

$$\begin{aligned}\frac{\partial^2\Delta_i}{\partial n_1\partial n_2} &= 4G_{i2}^{\ m1}\frac{1}{E}G_{m1}^{\ 12} - 2G_{ij}^{\ 12}\frac{1}{E}G_{ij}^{\ 12} + 8G_{ij}^{\ m2}\frac{1}{E}G_{m2}^{\ n1}\frac{1}{E}G_{n1}^{\ ij}\\
&- 16G_{ij}^{\ mm'}\frac{1}{E^2}G_{mm'}^{\ n1}\frac{1}{E}G_{n1}^{\ ij}\frac{\partial\Delta_i}{\partial n_2} + 2G_{ij}^{\ mm'}\frac{1}{E^2}G_{mm'}^{\ nn'}\frac{1}{E^2}G_{nn'}^{\ ij}\left(\frac{\partial\Delta_i}{\partial n_1}+\frac{\partial\Delta_j}{\partial n_1}\right)\left(\frac{\partial\Delta_i}{\partial n_2}+\frac{\partial\Delta_j}{\partial n_2}\right)\\
&- 2G_{ij}^{\ mm'}\frac{1}{E^3}G_{mm'}^{\ ij}\left(\frac{\partial\Delta_i}{\partial n_1}+\frac{\partial\Delta_j}{\partial n_1}\right)\left(\frac{\partial\Delta_i}{\partial n_2}+\frac{\partial\Delta_j}{\partial n_2}\right) - 2G_{i2}^{\ mm'}\frac{1}{E^2}G_{mm'}^{\ i2}\left(\frac{\partial\Delta_i}{\partial n_1}+\frac{\partial\Delta_2}{\partial n_1}\right)\\
&+ 4G_{ij}^{\ m1}\frac{1}{E^2}G_{m1}^{\ ij}\left(\frac{\partial\Delta_i}{\partial n_2}+\frac{\partial\Delta_j}{\partial n_2}\right) - G_{ij}^{\ mm'}\frac{1}{E^2}G_{mm'}^{\ ij}\left(\frac{\partial^2\Delta_i}{\partial n_1\partial n_2}+\frac{\partial^2\Delta_j}{\partial n_1\partial n_2}\right)\,.\end{aligned} \tag{A9}$$

We now have a closed system of equations, which are approximately solved in the text.

---

*Work supported in part by the U.S. Atomic Energy Commission and the Higgins Scientific Trust Fund.

[1]L. D. Landau, Zh. Eksperim. i Teor. Fiz. 30, 1058 (1956); 32, 59 (1957) [English transls.: Soviet Phys. – JETP 3, 920 (1957); 5, 101 (1957)].

[2]K. A. Brueckner and J. L. Gammel, Phys. Rev. 109, 1040 (1958); K. A. Brueckner, T. Soda, P. Anderson, and D. Morel, *ibid.* 118, 1442 (1966).

[3]E. Østgaard, Phys. Rev. 170, 257 (1968).
[4]T. Burkhardt, Ann. Phys. (N. Y.) 47, 516 (1968).
[5]H.-T. Tan and E. Feenberg, Phys. Rev. 176, 370 (1968).
[6]D. Pines and P. Nozieres, The Theory of Quantum Liquids (W. A. Benjamin, Inc., New York, 1966), see Eqs. (1.43), (1.61), and (1.67).
[7]N. F. Berk and J. R. Schrieffer, Phys. Letters 17, 433 (1966); S. Doniach and S. Engelsberg, *ibid.* 18, 750 (1966).
[8]J. Schrieffer and N. Berk, Phys. Letters 24A, 604 (1967).
[9]Functional differentiation is used in a related context to derive consistent theories in G. Baym and L. Kadanoff, Phys. Rev. 124, 287 (1961).
[10]Reference 2 and K. A. Brueckner and J. L. Gammel, Phys. Rev. 121, 1863(E) (1961). Brueckner's expression for the dependence of the G matrix on the Fermi momentum is numerically incorrect. The author thanks E. Østgaard and S. O. Bäckman for calling his attention to this point.
[11]A. J. Leggett and M. J. Rice, Phys. Rev. Letters 20, 586 (1968).
[12]G. A. Brooker, Proc. Phys. Soc. (London) 90, 397 (1967).
[13]R. Rajaraman and H. A. Bethe, Rev. Mod. Phys. 39, 745 (1967).
[14]Due to an error in Eq. (2.17) Ref. 3, Østgaard does not find self-consistency for these hole-energy parameters.
[15]The author thanks G. E. Brown and J. R. Schrieffer for emphasizing these points.
[16]V. J. Emery, Phys. Rev. 170, 205 (1968).
[17]D. J. Amit, J. W. Kane, and H. Wagner, Phys. Rev. 175, 313 (1968).
[18]N. Hugenholtz and L. Van Hove, Physica 24, 363 (1958).
[19]B. H. Brandow, Rev. Mod. Phys. 39, 771 (1967).
[20]In Ref. 3, Østgaard quotes half this value, as he does not include exchange.
[21]C. W. Wong, Nucl. Phys. 71, 389 (1968); G. Dahll, E. Østgaard, and B. Brandow, *ibid.* A124 481 (1969).
[22]K. A. Brueckner and D. T. Goldman, Phys. Rev. 117, 207 (1960), see Eq. (15).

PHYSICAL REVIEW VOLUME 184, NUMBER 1 5 AUGUST 1969

Quantum Theory of Hydrodynamic Currents*

D. D. H. Yee
Department of Physics, Polytechnic Institute of Brooklyn, Brooklyn, New York 11201
(Received 28 April 1969)

The current-current commutation relations, satisfied by the microscopic currents, are used to determine the algebraic properties of the basic hydrodynamic variables in quantum hydrodynamics. Using a Hamiltonian as suggested by the microscopic theory, a new system of hydrodynamic equations is obtained which contained the classical hydrodynamic equations including vortex motion in the classical limit. The concept of the fluid velocity in quantum mechanics of many particles is also discussed.

I. INTRODUCTION

Recently, Dashen and Sharp[1] have discussed the possibility of formulating relativistic-field theories in terms of currents. In other words, currents themselves are treated as fundamental dynamical variables rather than the underlying canonical fields. The motivations for initiating such a program are due to the success of current algebra in correlating the various properties of hadron physics. As a starting point of this method, they used the nonrelativistic quantum-field problem as a guide. In particular, the Hamiltonian can be rewritten in terms of currents by using a formal procedure. The substitutes for the equal time canonical commutation relations are the equal time commutation relations among currents which then provide a complete dynamical theory. The main emphasis of this type of theory is the algebraic structure of the equal time current-current commutation relations.

As pointed out by Dashen and Sharp, the use of currents as coordinates are not new for nonrelativistic problems especially in hydrodynamics. On the other hand, we find that the implications of the algebraic structure of the equal time current-current commutation relations satisfied by the microscopic currents had not been fully explored in quantum hydrodynamics. Unlike the problems in hadron physics, a hydrodynamic sys-